Magnetic Field Dependence of the Microwave Properties of Proximity Effect Nb/Al Bilayers Close to the Gap-frequency

S. Zhu, T. Zijlstra, C. F. J. Lodewijk, A. Brettschneider, M. van den Bemt, B. D. Jackson, A. M. Baryshev, A. A. Golubov, and T. M. Klapwijk

Abstract— High critical current density tunnel barriers of AlN have two effects on the operation of niobium-based SIS mixers close to the upper frequency limit of superconducting niobium: 1. the bandwidth is no longer limited by the RC time constant of the tunnel-junction, but the physical processes in the superconductors at high frequencies; 2. the devices have smaller lateral dimensions in order to provide impedance matching given the low R_nA value, which requires the application of a higher magnetic field to quench the Josephson-effect through the Fraunhofer pattern. Consequently, under operating conditions the superconducting properties are no longer the equilibrium properties as realized by the fabrication conditions, but are deteriorated by the applied magnetic field. We report the measurements of I-V curves and Fourier transmission spectrum to determine and correlate the evolution of the superconducting properties in a high magnetic field. The results are compared with a calculation of the proximity effect based on the Keldysh Greens' function technique, leading to a magnetic field dependent density of states in the Al toplayer of the commonly used Nb-Al bilayer to fabricate tunnel barriers as well as forming one part of the superconducting stripline.

***Index Terms*— Fourier transmission spectrum, gap frequency, magnetic field, proximity effect**

I. Introduction

Superconductor-insulator-superconductor (SIS) mixers for the ALMA Band-9 project (frequency range from 602 to 720 GHz) have been realized using the recently developed AlN technology. The epitaxial crystalline nature of the AlN barriers of the SIS junctions makes the distribution of tunnel-transmissivities much more narrow leading to good quality tunnel-junctions with an achievable critical current density, J_c, of up to 400 kA/cm^2 [1], much larger than those reported for amorphous AlO_x barriers [2]. The most beneficial contribution of high J_c junctions is that a larger bandwidth can be achieved due to the lower R_nC_j time constant with R_n the normal state resistance and C_j the junction capacitance (provided the matching circuit is not limiting [3]). Because of the lower specific resistance, R_nA value, of the barrier, the junction area, A, should be smaller to provide the desired impedance matching.

In the junction fabrication, the AlN barrier is produced by depositing about 7-8 nm Al layer on a 200 nm Nb ground plane, followed by a nitridation of the Al layer in a nitrogen plasma for a fixed time to form an insulating barrier with a thickness of about 1 nm. The final structure of the SIS junction is Nb/Al/AlN/Nb and the corresponding tuning circuit is Nb/Al/AlN/SiO_x/Nb multilayer, as illustrated in Fig. 1. The thickness of SiO_x is 250 nm and top Nb 500 nm. Here the tuning circuit is, as usual, employed to match the antenna impedance with the SIS junction impedance.

From the point of view of applications the higher J_c and lower A of the junction mean also that a higher magnetic field has to be applied to suppress the Josephson current, which shows a Fraunhofer pattern with the magnetic field. As a consequence, the superconducting properties, especially for the Nb/Al ground plane, are no longer in the equilibrium state, but are deteriorated by the magnetic field. Technologically, it is of interest to investigate the influence of magnetic field on the electrodynamics of the tuning circuit in the SIS mixer. The superconductivity of the proximity-coupled Nb/Al bilayer is potentially dependent on the external field, in particular for frequencies close to the gap frequency.

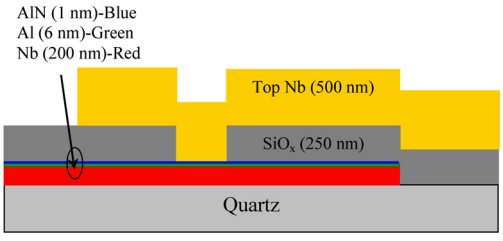

Fig. 1. Cross-section of the SIS junction and tuning circuit. Proximity effect can be directly observed in the I-V measurements of the junction. Transmission efficiency of the Nb/Al ground plane is correlated with the I-V curves and magnetic fields.

II. Proximity Effect Model

The proximity effect has been studied theoretically and

Manuscript received 20 April 2009. This work was supported in part by NanoImpuls, the Dutch Research School for Astronomy (NOVA), the Dutch Organization for Scientific Research (NWO), Radionet, and the European Southern Observatory (ESO).

S. Zhu, T. Zijlstra, C. F. J. Lodewijk, A. Brettschneider, and T. M. Klapwijk are with the Kavli Institute of Nanoscience, Faculty of Applied Sciences, Delft University of Technology, Lorentzweg 1, 2628 CJ Delft, The Netherlands (corresponding author to provide phone: 0031-15-2786113; e-mail: s.zhu@tudelft.nl).

M. van den Bemt, B. D. Jackson, A. M. Baryshev are with SRON National Institute for Space Research, 9747 AD Groningen, The Netherlands.

A. A. Golubov is with Faculty of Science & Technology, University of Twente, 7500 AE Enschede, The Netherlands.

experimentally in the past twenty years [4]-[6]. When a normal metal N is electrically in contact with a superconductor S, the properties of both S and N are altered. A model applicable to our samples has been developed by Golubov *et. al*. to deal with the proximity-coupled S/N bilayer in the dirty limit condition [4], also in the presence of a magnetic field. Considering the polycrystalline of Nb and Al layers deposited using the sputtering technique at room temperature, this dirty limit condition also holds for our samples.

The Usadel equations [7], describing the inhomogeneous state of a dirty superconductor in the weak-coupling limit, can be rewritten in a so-called θ-parameterized way [5]:

$$\xi^2 \frac{\partial^2}{\partial x^2}\theta(x) + j\varepsilon \sin[\theta(x)] + \Delta(x)\cos[\theta(x)] = 0, \tag{1a}$$

$$\Delta(x)\ln\frac{T}{Tc} + 2\frac{T}{T_C}\sum_{\omega_n}\left(\frac{\Delta(x)}{\omega_n} - \sin[\theta(x)]\right) = 0, \tag{1b}$$

where θ is a unique Green functions, ξ the coherence length, ε the quasi-particle energy, and $\omega_n=\pi T(2n+1)$ $(n=0,1,2,...)$ the Matsubara frequency. The quasi-particle density of state can be defined as

$$\frac{N(E)}{N(0)} = \mathrm{Re}[\cos(\theta)]. \tag{2}$$

For the proximity-coupled S/N bilayer, (1) can be used to describe the S and N layers, respectively, with the boundary conditions at the S-N interface:

$$\xi_S \frac{\partial}{\partial x}\theta_S(x) = \gamma\xi_N \frac{\partial}{\partial x}\theta_N(x), \gamma = \rho_S\xi_S / \rho_N\xi_N, \tag{3a}$$

$$\gamma_{BN}\xi_N \frac{\partial}{\partial x}\theta_N(x) = \sin[\theta_S(x) - \theta_N(x)], \gamma_{BN} = R_B / \rho_N\xi_N, \tag{3b}$$

as well as at the free surface of both S and N layers:

$$\frac{\partial}{\partial x}\theta(d_S) = 0, \tag{4a}$$

$$\frac{\partial}{\partial x}\theta(-d_N) = 0, \tag{4b}$$

where γ and γ_{BN} are the interface parameters describing the nature of the interface between the S and N layers, $\rho_{S,N}$ denote the normal state resistivities, R_B is the product of the resistance at S/N interface and its area, and $d_{S,N}$ the thickness of S and N layer, respectively. When a weak magnetic field is applied, an extra energy term related to the orbital effect can be added to the quasi-particle energy in (1a) as $\varepsilon+j\Gamma\cos[\theta(x)]$. Here, $\Gamma=(H\xi W/\Phi_0)^2\pi^{1/3}$ is the effective pair-breaking rate and H is the magnetic field, ξ the coherence length of S layer, W the thickness of bilayer, and Φ_0 the flux quantum [8].

To numerically solve (1), we set the interface parameters γ and γ_{BN} as 0.5 and 0.7, respectively, both of which have been experimentally determined by Zehnder *et.al.* for the Nb/Al SNINS junction with 200 nm Nb and 4 nm Al layers [6]. These values are also very close to the ones (γ=0.3 and γ_{BN} =1.0) reported by Dmitiriev *et. al.* without considering the film thickness [9]. The other input parameters, such as temperature and film thickness, can be set according to the details of the experiment.

Fig. 2 shows the calculated density of state at four typical positions, *i.e.*, the free surfaces and interfaces of Nb and Al layer, in two different magnetic fields. It can be observed that the curves for the density of states at these typical positions in the same field are almost identical except for a slight difference at the free surface position of the Nb layer when d_{Nb} (200 nm)>>d_{Al} (6 nm). This means that the very thin Al layer has similar superconducting properties as the thick Nb layer. As a rough, but reasonable, approximation, the Nb/Al bilayer can be treated as a single layer with uniform superconducting properties. For thicker films the properties become inhomogeneous [4]-[6].

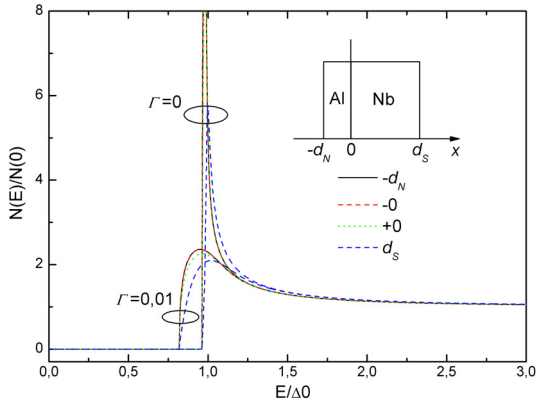

Fig. 2. Density of states at four typical positions inside the proximity-coupled Nb/Al bilayer. The thicknesses of Nb and Al layer are 200 nm and 6 nm, respectively. Δ0 is the calculated gap energy of bulk Nb superconductor, which is normalized to $\pi k_B T_{CS}$, T_{CS}=9.27 K. Γ is the pair-breaking rate defined in [8]. Inset shows the sketch of the Nb/Al bilayer.

III. Surface Impedance

The electromagnetic behavior of a uniform superconductor is described by the Mattis-Bardeen theory [10]. The application to a proximity-layer is usually done by assuming full Nb superconducting properties throughout the Al. It has been shown, at the low frequency of about 10 GHz, that only for thick enough Al (tens of nanometers) the surface impedance of the Nb/Al bilayers begins to deviate from those of bare Nb samples [11]. In our case, with the frequency close to the gap frequency of Nb (~680 GHz), it is likely that similar deviations will occur already for thinner Al layers.

In order to describe the microwave response of the Nb/Al bilayer, we use the reformulation of Mattis-Bardeen proposed by Nam. It is a more general theory that can be applied to the strong-coupling and to the impure superconductors [12]. We calculate the complex conductivity, $\sigma/\sigma_N=(\sigma_1-j\sigma_2)/\sigma_N$, of the proximity-coupled Nb/Al bilayer by assuming an uniform superconductivity in the bilayer.

Nam's equations for the complex conductivity calculation in the dirty limit read as [12]:

$$\frac{\sigma_1}{\sigma_N} = \frac{1}{\hbar\omega}\int_{\Delta-\hbar\omega}^{-\Delta} g_1(1,2)\tanh[\frac{1}{2k_BT}(\hbar\omega+E)]dE + \frac{1}{\hbar\omega}\int_{\Delta}^{\infty} g_1(1,2)\{\tanh[\frac{1}{2k_BT}(\hbar\omega+E)] - \tanh(\frac{1}{2k_BT}E)\}dE, \tag{5a}$$

$$\frac{\sigma_2}{\sigma_N} = \frac{1}{\hbar\omega}\int_{\Delta-\hbar\omega}^{\Delta} g_2(1,2)\tanh[\frac{1}{2k_BT}(\hbar\omega+E)]dE + \frac{1}{\hbar\omega}\int_{\Delta}^{\infty}\{g_2(1,2)\tanh[\frac{1}{2k_BT}(\hbar\omega+E)] + g_2(2,1)\tanh(\frac{1}{2k_BT}E)\}dE \tag{5b}$$

Here the functions $g_{1,2}$ are known as coherence factor and given

by:

$$g_1(1,2) = \mathrm{Re}[N(1)]\mathrm{Re}[N(2)] + \mathrm{Re}[P(1)]\mathrm{Re}[P(2)], \quad (6a)$$

$$g_2(1,2) = \mathrm{Im}[N(1)]\mathrm{Re}[N(2)] + \mathrm{Im}[P(1)]\mathrm{Re}[P(2)], \quad (6b)$$

where N and P denote the density of state and pairs as calculated from (1), and the arguments 1, 2 represent the quasi-particle energy of E and $E+\hbar\omega$. The gap energy, Δ, can be derived from the density of states as shown in Fig. 2 and the normal state conductivity, σ_N, as evaluated experimentally.

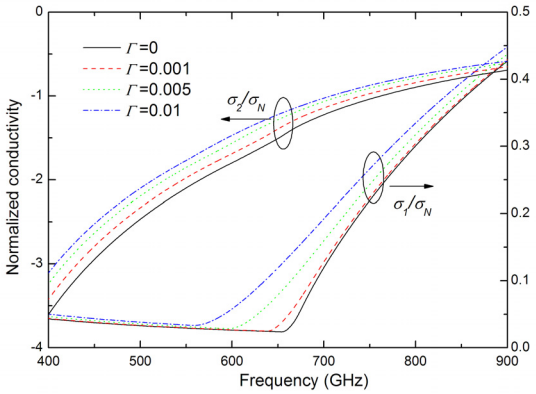

Fig. 3. Dependence of the complex conductivity on the frequency at different magnetic fields. The densities of state and pairs of surface of Al layer are used to calculate the complex conductivity.

Fig. 3 shows the calculated complex conductivity of the bilayer. It can be seen that the gap frequency of the Nb/Al bilayer is about 650 GHz and can be further suppressed by the magnetic field. The absolute value of the imaginary part of complex conductivity, which is related to the paired electrons, decreases, while the real part contributed by the quasi-particles increases when the magnetic field is increased, which indicates the pair-breaking role of the magnetic field.

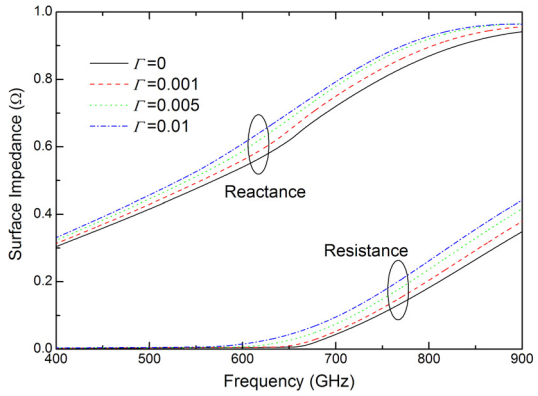

Fig. 4. Calculated surface impedance of the Nb/Al bilayer according to (7). The normal state conductivity σ_N is 1.0×10^7 *S/m*.

When the electric field penetration depth is long compared to the electron mean free path, a local equation can be assumed for the relation between the current density, J, and the electrical field, E, as $J=\sigma E$, where σ is the complex conductivity. If the thickness d of a conductor is not very much greater than the penetration depth, the field at one side of the conductor penetrates partially into the film. In this case, the normal skin effect surface impedance is found by solving Maxwell's equations in the local limit [13]:

$$Z_S = \sqrt{\frac{j\omega\mu_0}{\sigma}}\coth(d\sqrt{j\omega\mu_0\sigma}). \quad (7)$$

By substituting the calculated complex conductivity in (7), one can get the surface impedance of the Nb/Al bilayer as shown in Fig. 4. Here the normal state conductivity is set as $\sigma_N = 1.0\times10^7$ *S/m* and the thickness of the bilayer is 200 nm. Both the surface resistance and the reactance increase with magnetic field, which means that more losses will be introduced in the transmission line (tuning circuit). It can be expected that the Fourier transform spectrometer (FTS) response of the mixer would be depressed by the magnetic field, as discussed in a very similar situation, *i.e.*, the anodization process [3].

IV. I-V Curves and FTS Response in Magentic Field

I-V measurement can provide some important information about the quality of the superconducting films, although they do not directly provide the information about the quality of the materials forming the tuning circuit. It is well known that there is a characteristic "knee" structure in the I-V curves of a SNINS or SNIS junction, which can be explained in the framework of the proximity-effect theory [4]. We have measured the DC I-V curves of the SIS mixer at 4.2 K in different magnetic fields. The magnetic field is generated by a superconducting magnet-coil, and its value is determined from the applied coil current, I_m.

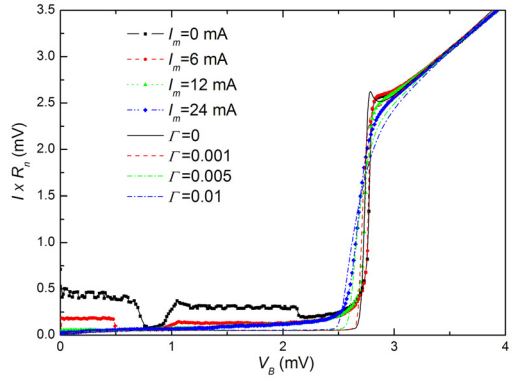

Fig. 5. Measured (symbols) and calculated (lines) I-V curves of the SIS junction at different magnetic fields. The product of I and R_n is used to represents the tunnel current. The measured value of R_n is 18 Ω. The calculation shows a lower V_g than the measurements.

As shown in Fig. 5, the Josephson current is suppressed by the magnetic field, while the gap voltage and the sharp non-linearity at the gap get also depressed at sufficiently high magnetic fields. Using the calculated density of states at the free surface of Al layer, we compare the measured I-V curves with the calculated ones. It is seen that the calculations are qualitatively in agreement with the measurements, *i.e.*, the "knee" structure disappears and the gap voltage is reduced while the nonlinearity at the gap weakens. The Josephson current is not included in the calculation. It also should be mentioned that the calculated V_g, for the given set of parameters, is smaller than the one determined from the measurements. The measured V_g can be up to 2.77 mV, while the calculated result is only 2.74 mV for the Nb bulk and 2.64 mV for the Nb/Al bilayer.

The multi-section Nb/Al/AlN/SiO_2/Nb microstripline is used to tune out the junction capacitance and transfer the RF signal

from the probe point to the junction. The transmission efficiency of the microstripline is evaluated using a FTS setup by measuring the changes in the DC current produced by the incoming radiation at a bias voltage of 2.0 mV. The SIS device is mounted in a waveguide backpiece and the FTS setup is operated in air, which leads to water vapor absorption at the edges of the band.

The FTS data are taken at 4.2 K as shown in Fig. 6. A good FTS response is obtained over the full desired band (602-720 GHz). The minima in the response at 560 and 750 GHz are due to the absorption of water vapor in the atmosphere. The magnetic field is applied to suppress the Josephson current during the measurement. It is observed that the FTS response decreases with the increase of the magnetic field when the frequency is between 630 and 730 GHz. We suggest that, since the magnetic field has less influence on the top Nb wire, it should result from the deteriorated superconductivity of the Nb/Al ground plane. As discussed in section III, when the magnetic field is applied, the bilayer shows a lower gap energy and a higher surface impedance at frequencies higher than the gap frequency. Based on the transmission line theory [14], the lower gap energy means a lower frequency cut-off and higher surface resistance leads to increased losses in the tuning circuit, *i.e.*, smaller transmission efficiencies.

We have calculated the transmission efficiencies and the results are shown in Fig. 6. The fitting parameters are: $R_nA=9.8\ \Omega.\mu m^2$, $C_j=60\ fF/\mu m^2$, $\sigma_N=0.9\times10^7\ S/m$, and dielectric constant of SiO_x $\varepsilon=4.8$. The complex conductivity of the top Nb layer is calculated using the Mattis-Bardeen equations [10], and the V_g of top Nb layer is 2.8 mV. The 80% absorption of the atmosphere is also considered in the calculation. It is seen that the calculated FTS decreases with the increase of the magnetic field, but less dramatically than the measured result. The reason of this difference in sensitivity should be further explored.

We also like to argue that this calculation is justified in the case that the Pippard coherence length is much larger than the penetration depth. For a more detailed description of the Nb-based superconducting microstripline above the gap frequency, the full Mattis-Bardeen, or Nam, theory could be used, as pointed out by Pöpel [15].

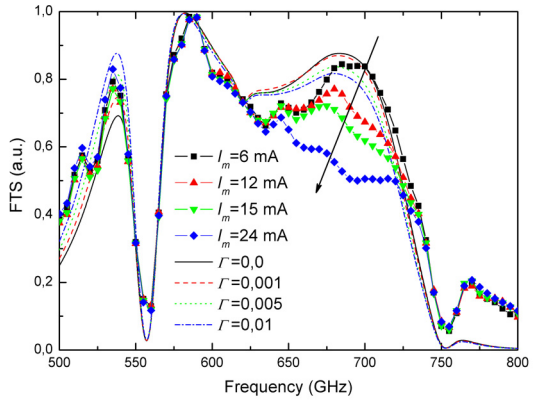

Fig. 6. Measured (symbols) and calculated (lines) FTS response of the SIS mixer with different magnetic fields. Each curve has been normalized to its max value. The calculation shows less sensitivity to the variation of magnetic field compared to the measurement.

V. Conclusion

We have analyzed the influence of the magnetic field on the transmission efficiency of a Nb/Al/AlN/SiO_x/Nb tuning circuit of the SIS mixer for the ALMA Band-9 project. Both the calculations and the measurements clearly indicate a significant deterioration of the FTS response with the applied magnetic field when frequency is close to the gap frequency of the proximity-coupled Nb/Al bilayer. This deterioration can be qualitatively described by the proximity theory of S/N bilayer and the electrodynamics of inhomogeneous superconductor.

The observed magnetic field dependence of the FTS response also exists in the SIS mixers with AlO_x barrier. However, due to the relatively low J_c and large A, the magnetic field used to suppress the Josephson current is small and this behavior can usually be ignored. To avoid the depression of FTS response in magnetic field, we suggest that a light anodization-step could be used to make the metallic Al layer into insulating AlO_x layer in the tuning circuit.

References

[1] T. Zijlstra, C. F. J. Lodewijk, N. Vercruyssen, F. D. Tichelaar, D. N. Loudkov, and T. M. Klapwijk, "Epitaxial aluminium nitride tunnel barriers grown by nitridation with a plasma source," Appl. Phys. Lett., vol 91, Dec. 2007, pp. 233102-1-3.

[2] R. E. Miller, W. H. Mallison, A. W. Kleinsasser, K. A. Delin, and E. M. Macedo, "Niobium trilayer Josephson tunnel junctions with ultrahigh critical current densities," Appl. Phys. Lett., vol 63, Sep. 1993, pp. 1423-1425.

[3] C. F. J. Lodewijk, T. Zijlstra, S. Zhu, F. P. Mena, A. M. Baryshev, and T. M. Klapwijk, "Bandwidth limitations of Nb/AlN/Nb SIS mixers around 700 GHz," IEEE Trans. Appl. Supercond., to be published.

[4] A. A. Golubov, E. P. Houwman, J. G. Gijsbertsen, V. M. Krasnov, J. Flokstra, H. Rogalla, and M. Yu. Kupriyanov, "Proximity effect in superconductor-insulator-superconductor Josephson tunnel junctions: theory and experiment," Phys. Rev. B, vol 51, Jan. 1995, pp. 1073-1089.

[5] G. Brammertz, A. A. Golubov, A. Peacock, P. Verhoeve, D. J. Goldie, R. Venn, "Modelling the energy gap in transition metal/aluminium bilayers," Physica C: Superconductivity, vol 350, Feb. 2001, pp. 227-236.

[6] A. Zehnder, Ph. Lerch, S. P. Zhao, Th. Nussbaumer, E. C. Kirk, and H. R. Ott, "Proximity effects in Nb/Al-AlO_x-Al/Nb superconducting tunnel junctions," Phys. Rev. B, vol 59, Apr. 1999, pp. 8875-8886.

[7] K. D. Usadel, "Gerneralized diffusion equation for superconducting alloys," Phys. Rev. Lett., vol 25, Aug. 1970, pp. 507-509.

[8] W. Belzig, C. Bruder, and Gerd Schön, "Local density of states in a dirty normal metal connected to a superconductor," Phys. Rev. B, vol 54, Oct. 1996, pp. 9443-9448.

[9] P. N. Dmitiriev, A. B. Ermakov, A. G. Kovalenko, V. P. Koshelets, N. N. Iosad, A. A. Golubov, M. Yu. Kupriyanov, "Niobium tunnel junctions with multi-layered electrodes," IEEE Trans. Appl. Supercond., vol 9, Jun. 1999, pp. 3970-3973.

[10] D. C. Mattis and J. Bardeen, "Theory of the anomalous skin effect in normal and superconducting metals," Phys. Rev., vol 111, Jul. 1958, pp. 412-417.

[11] M. S. Pambianchi, S. N. Mao, and S. M. Anlage, "Microwave surface impedance of proximity-coupled Nb/Al bilayer films," Phys. Rev. B, vol 52, Aug. 1995, pp. 4477-4480.

[12] S. B. Nam, "Theory of electromagnetic properties of superconducting and normal systems," Phys. Rev., vol 156, Apr. 1967, pp. 470-486.

[13] R. L. Kautz, "Picosecond pulses on superconducting stripelines," J. Appl. Phys., vol 49, Jan. 1978, pp. 308-314.

[14] G. de Lange, J. J. Kuipers, T. M. Klapwijk, R. A. Panhuyzen, H. van de Stadt, and M. W. M. de Graauw, "Superconducting resonator circuits at frequencies above the gap frequency," J. Appl. Phys., vol 77, Feb. 1995, pp 1795-1804.

[15] R. Pöpel, "Surface impedance and reflectivity of superconductors", J. Appl. Phys., vol 66, Dec. 1989, pp. 5950-5957.